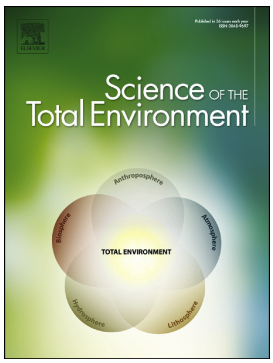

In vivo assessment of silver nanoparticle induced reactive oxygen species reveals tissue specific effects on cellular redox status in the nematode Caenorhabditis elegans

Lisa M. Rossbach, Deborah H. Oughton, Erica Maremonti, Claire Coutris, Dag A. Brede

PII: S0048-9697(20)31176-1

DOI: https://doi.org/10.1016/j.scitotenv.2020.137665

Reference: STOTEN 137665

To appear in: *Science of the Total Environment*

Received date: 15 November 2019

Revised date: 26 February 2020

Accepted date: 29 February 2020

Please cite this article as: L.M. Rossbach, D.H. Oughton, E. Maremonti, et al., In vivo assessment of silver nanoparticle induced reactive oxygen species reveals tissue specific effects on cellular redox status in the nematode Caenorhabditis elegans, *Science of the Total Environment* (2020), https://doi.org/10.1016/j.scitotenv.2020.137665

In vivo assessment of silver nanoparticle induced reactive oxygen species reveals tissue specific effects on cellular redox status in the nematode *Caenorhabditis elegans*

Lisa M. Rossbach[1,*], Deborah H. Oughton[1], Erica Maremonti[1], Claire Coutris[2] and Dag A. Brede[1]

[1]Norwegian University of Life Sciences, Faculty of Environmental Sciences and Natural Resource Management, P.O. BOX 5003 NMBU, No-1432 Ås, Norway

[2]Norwegian Institute of Bioeconomy Research, Division of Environment and Natural Resources, Høgskoleveien 7, Ås, Norway

*Corresponding author: Lisa.rossbach@nmbu.no

Abstract

The current study provides an *in vivo* analysis of the production of reactive oxygen species (ROS) and oxidative stress in the nematode *Caenorhabditis elegans* following exposure to EU reference silver nanoparticles NM300K and $AgNO_3$. Induction of antioxidant defenses was measured through the application of a SOD-1 reporter, and the HyPer and GRX biosensor strains to monitor changes in the cellular redox state. Both forms of Ag resulted in an increase in *sod-1* expression, elevated H_2O_2 levels and an imbalance in the cellular GSSG/GSH redox status. Microscopy analysis of the strains revealed that $AgNO_3$ induced ROS-related effects in multiple tissues, including the pharynx, intestinal cells and muscle tissues. In contrast, NM300K resulted in localized ROS production and oxidative stress, specifically in tissues surrounding the intestinal lumen. This indicates that Ag from $AgNO_3$ exposure was readily transported across the whole body, while Ag or ROS from NM300K exposure was predominantly confined within the luminal tissues. Concentrations resulting in an increase in ROS production and changes in GSSG/GSH ratio were in line with the levels associated with observed physiological toxic effects. However, *sod-1* was not induced at the lowest Ag concentrations, although reprotoxicity was seen at these levels. While both forms of Ag caused oxidative stress, impaired development, and reprotoxicity, the results suggest different involvement of ROS production to the toxic effects of $AgNO_3$ versus NM300K.

Keywords: reporter strain, biosensor strain, oxidative stress, NM300K

1. Introduction

Due to their wide applications, silver nanoparticles (Ag NPs) are one of the most intensively studied nanomaterials available (Syafiuddin et al., 2017). Characteristics, such as size, surface charge, chemistry, and dissolution state of the NPs can influence bioavailability, reactivity and toxicity of the material (Foldbjerg et al., 2009, Zhao and Wang, 2011, Völker et al., 2015). The EU reference material NM300K has been provided by the European Commission Joint Research Centre and is one of the best characterized Ag NPs available (Wasmuth et al., 2016, Köser et al., 2017). Furthermore, the toxicity of NM300K has been assessed in a wide range of species, such as bacteria, daphnia, annelids (Poynton et al., 2012, van der Ploeg et al., 2014, Ribeiro et al., 2015, Gomes et al., 2017), and the nematode *Caenorhabditis elegans* (Kleiven et al., 2018). Results from Kleiven et al. (2018) show distinct differences in toxicity between $AgNO_3$ and the Ag NP NM300K, with higher retention of Ag from $AgNO_3$ following the depuration of the nematodes. These differences have been supported by a follow-up study on multigenerational effects Ag NPs versus $AgNO_3$, which also suggests a clear difference in the toxic mode of action between the two forms of Ag (Rossbach et al., 2019).

Silver nanoparticles have been shown to induce physical damages to the cuticle of *C. elegans* (Kim et al., 2012), and negatively affect physiological processes, including reproduction and development. At the molecular level, Ag NPs interfere with metabolism by inhibition of enzyme activities, which may damage cellular constituents including

mitochondria and DNA (Nel et al., 2006, Kim et al., 2009, Roh et al., 2009, Piao et al., 2011). Moreover, one of the most important toxic mechanisms of Ag NPs is the production of free radicals on the surface of the particle, which may impact biological molecules and cellular structures, potentially leading to oxidative stress (Kim et al., 2009, Roh et al., 2009, Lüersen et al., 2013, Ribeiro et al., 2015).

A range of studies highlight differences in toxic mechanism between ionic Ag and Ag NPs (Hunt et al., 2013, Choi et al., 2018), possibly explained by differences in reactive oxygen species (ROS) formation and oxidative stress development between the two forms of Ag (McShan et al., 2014). Lim et al. (2012) highlight the importance of ROS formation by Ag NPs in *C. elegans* and suggest that oxidative stress plays an important role in Ag NP reproductive toxicity, whereas $AgNO_3$ exposure did not result in a significant increase in ROS. A study in the soil organism *Enchytraeus crypticus* showed distinct differences in the oxidative stress defense mechanisms and response patterns between the Ag NPs NM300K and $AgNO_3$ (Ribeiro et al., 2015). Comparatively, it has been shown that any oxidative stress measured following the exposure of *Daphnia magna* to either Ag NPs or $AgNO_3$, could almost entirely be attributed to ionic releases from the NPs, due to similar response patterns from the two forms of Ag (Li et al., 2015).

Due to extensive knowledge about its biology and physiology, the nematode *C. elegans* is an excellent model organism for studying ROS production, and oxidative stress mechanisms. Studies suggest that *C. elegans* possesses a highly complex, but nevertheless specialized, ROS and redox control system (Braeckman et al., 2016). For instance, their genomes encode for five superoxide dismutase (SOD) forms, used for the detoxification of

superoxides, with SOD-1, SOD-4 and SOD-5 being Cu/ZnSOD isoforms, while SOD-2 and SOD-3 are mitochondrial MnSOD isoforms (McCord and Fridovich, 1969, Braeckman et al., 2016). SOD-1, is localized in the cytosol and mitochondrial intermembrane space, is evenly expressed and is responsible for ~75% of total SOD activity in *C. elegans* (Doonan et al., 2008). *C. elegans* oxidative stress defense includes multiple catalase (CTL) and glutathione peroxidase (GPX) enzymes. Under normal conditions, glutathione molecules are mostly reduced, with only a low proportion of the oxidized glutathione disulphide (GSSG) present (Lüersen et al., 2013). Elevated ROS thus leads to expenditure of GSH with the production of GSSG. The NADPH-dependent GSSG reductase (GSR) recycles of excess GSSG into GSH (Lüersen et al., 2013). Furthermore, y-glutamylcysteine synthetase (GCS) and GSH synthetase (GSS) contribute to maintain GSH/GSSG homeostasis (Townsend et al., 2003, Lüersen et al., 2013). Hence, due to the high intracellular abundance of this redox couple, the quantification of changes in the GSSG/GSH ratios allows for a reliable indication of the total redox state of the cell (Schafer and Buettner, 2001, Braeckman et al., 2016, Braeckman et al., 2017).

Through the use of a reporter strain SOD-1 (GA508 wuls54[pPD95.77 sod-1::GFP, rol-6(su1006)]) and two biosensors HyPer and Grx1-roGFP2 (GRX), the current study aimed to elucidate changes in the intracellular redox state in response to either $AgNO_3$ or NM300K Ag NP exposure, by the nematode *C. elegans*, and relate these findings to standard toxicity test endpoints. It was hypothesized that differences in the localization of oxidation signals by the strains would be governed by differences in retention and distribution of the Ag from the $AgNO_3$ and Ag NPs by *C. elegans*. Furthermore, building on the results of previous studies with *C. elegans* (Lim et al., 2012), it was hypothesized that ROS production would

elicit an antioxidant defense response to counteract oxidative stress and prevent adverse effects to growth, fertility and/or reproduction.

2. Methods

2.1. Nanoparticle stock preparation and characterization

The OECD representative Ag nanomaterial NM300K (Fraunhofer IME, Munich, Germany) stocks were prepared according to a Standard Operating Procedure developed by EU NanoReg (Jensen et al., 2016). Briefly, a 2.56 g Ag L^{-1} stock was prepared in ddH_2O (15 MΩ·cm) using a probe sonicator (Branson S-450 D sonicator, disruptor horn 13 mm) for 13 minutes at 15 % amplitude. Fresh stocks were prepared for each exposure.

For the characterization of the nanoparticles, a range of tools was employed. Dynamic light scattering (DLS, Malvern PN3702 Zetasizer Nanoseries) for hydrodynamic diameter and zeta potential, and transmission electron microscopy (TEM, Morgagni 268, FEI) for core diameter were carried out on stock solutions. For the TEM analysis, a 250 mg Ag L^{-1} stock was prepared in ddH_2O (15 MΩ·cm), before addition to the grid and subsequent TEM imaging.

Assessment of the size distribution and particle dissolution at T-0 and 72 h of exposure was carried out by ultrafiltration of the exposure media using 3 kDa Millipore Centrifugal filters (Amicon, Millipore). Triplicate samples of the exposure media were first centrifuged (2000 g for 5 min) to remove *E. coli* and larger particle aggregates, with subsequent ultrafiltration of the supernatants following pre-conditioning of the filters. For the dissolved (LMM) Ag

fraction, 400 µL of sample was added, and centrifuged at 14 000 g for 30 min, with a subsequent collection of 200 µL of the filtrate for analysis.

All samples were analyzed by Inductively Coupled Plasma Optical Emission Spectrometry (Agilent Technologies 5110 ICP-OES) or Mass Spectrometry (ICP MS Agilent 8800, Mississauga, Canada), using oxygen as a collision gas, and tuned using the manufacturer's tuning solution (#5188-6564, Agilent Technologies, Mississauga, Canada). Measurements were carried out on two Ag isotopes (107 and 109), with detection limits at 0.007 and 0.005 µg L^{-1}, respectively, and limits of quantification at 0.02 µg L^{-1}.

2.2. Nematode culture and exposure

All nematodes were exposed to either $AgNO_3$ or the silver nanoparticle NM300K in either 96 h (wild type N2), or 72 h (SOD-1, HyPer and GRX) standard toxicity tests, according to the International Organization for Standardization guideline 10872 (International Organization for Standardization, 2010), with some modification. Prior to the start of the exposure, nematodes, previously kept in liquid cultures, were treated with a hypochlorite solution for egg extraction and synchronization of the culture. Eggs were allowed to hatch on agar plates overnight to obtain synchronous L1-stage larvae.

2.3. Toxicity test exposure and sampling

All nematodes were exposed in 24-well culture plates, from L1 stage, at 20 °C in the dark, with continuous gentle shaking for sufficient oxygenation. Each well contained 1 mL of the bacteria *Escherichia coli* OP50 re-suspended in moderately hard reconstituted water (MHRW) (United States Environmental Protection Agency, 2002), and 11 ± 6 L1 stage

nematodes. Toxicity tests were carried out using the N2 Bristol strain, while ROS production and oxidative stress effects were assessed using one reporter and two biosensor strains.

The N2 Bristol strain *C. elegans* (*Caenorhabditis Genetic Centre*, Minneapolis, USA) was exposed in triplicate to nominal concentrations of 0.125, 0.25, 0.5, 1, 2 and 4 mg Ag L^{-1} for $AgNO_3$, or 1.25, 2.5, 5, 10, 20 and 40 mg Ag L^{-1} for NM300K Ag NPs. To terminate toxicity tests, 0.5 mL of Rose Bengal was added and toxicity test plates were kept for 10 minutes at 80 °C. A stereo microscope (Leica M205C) was used for assessment of growth, fertility and reproduction (International Organization for Standardization, 2010), using a hand held tally counter. The raw data obtained from this toxicity test have also been used as part of a multigenerational study studying the adaptive tolerance of *C. elegans* to NM300K Ag NPs (Rossbach et al., 2019).

Through the measurement of the emitted green fluorescent protein (GFP) signal, the SOD-1 strain (GA508 wuls54[pPD95.77 sod-1::GFP, rol-6(su1006)]) allows for a direct *in vivo* measurement of the induction of *sod-1* gene expression. The HyPer strain expresses a peroxide-specific sensor protein, consisting of a redox sensitive yellow fluorescent protein fused to the H_2O_2 sensing domain of *E. coli* OxyR (Back et al., 2012). The HyPer biosensor strain thus facilitates the *in vivo* quantitative assessment of H_2O_2 levels with cell specific resolution. When exposed to peroxide, an intramolecular disulfide bridge is formed which leads to a conformational change of the protein that results in the shift of the 420/500 nm excitation to 516 nm emission ratio. Similarly, the Grx1-roGFP2 (GRX) transgenic strain enables assessment of the ratio between the oxidized (GSSG) and reduced (GSH) forms of

glutathione (Back et al., 2012). In this manner, changes in the GRX emission ratio are directly determined by the GSSG/GSH ratio, and reflect the intracellular redox potential in the nematode. Quantification of the changes in GRX emission ratio thus provides information about the manifestation of oxidative stress (Back et al., 2012).

Due to slight differences in sensitivity of the reporter and biosensor strains compared to the wild type, lower concentration ranges were chosen of 0.1, 0.5 and 1 mg Ag L^{-1} for $AgNO_3$ or 1, 5 and 10 mg Ag L^{-1} for Ag NPs, in triplicate (with 10 nematodes per well). For sampling and analysis, 10 randomly selected nematodes from each exposure concentration were immobilized with 30 mM of sodium azide (NaN_3) and imaged using a fluorescent light microscope (LEICA DM6 B), equipped with a 405 nm excitation and 535 nm emission filter. For oxidized to reduced ratios of the biosensor strains, a second image (Ex 490 nm and Em 535 nm) was taken. Ratios were calculated as described in Back et al (2012). The SOD-1 average intensity was normalized to nematode total body length, to account for possible variation in signal strength due to developmental stages (Doonan et al., 2008). All images were quantified using the LAS X Leica application suit X imaging software for pixel based average intensity measurements.

To exclude possible interferences or enhancement of fluorescent signals by Ag NPs in nematodes, N2 nematodes exposed to Ag NPs were analyzed at both excitation (405 and 490 nm) and emission (525 nm) wavelengths, and signals were compared to control (unexposed) N2 nematodes (see supplementary materials, figure S3). Moreover, Ag NP suspensions were analyzed for fluorescence at both wavelengths.

2.4. Statistical analysis

For the statistical analysis of all the data, Minitab® 18 software was used. A significance level of 0.05 was used in all tests. Differences between treatments were analyzed using ANOVA, followed by a Tukey´s range test. Alternatively, a Kruskal-Wallis test was done when the residuals of the ANOVA were not normally distributed. For the comparison of the various nematode strains, a Spearman rank or Pearson product moment correlation test was used.

Effect concentrations (EC10 and EC50) were calculated with the open source software RegTox, using the Hill model (Vindimian, 2016) and are reported as the optimal value for EC10 and EC50 with corresponding 95 % confidence intervals.

3. Results

3.1. Nanoparticle characterization

Since the importance of physicochemical characteristics of Ag NPs in explaining toxic responses has been shown in previous studies (Kleiven et al., 2018), we conducted detailed characterization of the NM300K Ag NPs, prior and post application to the exposure media, as well as monitored changes over time. TEM analysis of stock suspensions showed an average size of 23.2 ± 17.2 nm (mean ± SD, throughout the text) (Figure S1), which is in good agreement with supplier characteristics. DLS analysis showed an average diameter of 93.3 ± 1.3 nm and 87.6 ± 1 nm and a PdI of 0.3 and 0.25, for the initial 256 mg Ag L^{-1} (Figure S2) and the diluted 100 mg Ag L^{-1} stocks in ddH_2O (15 MΩ·cm), respectively. The

measurement of the electrophoretic mobility of the Ag NPs in the stocks showed a zeta potential of -8.77 and -14.3 mV for the 256 and 100 mg Ag L^{-1} stocks, respectively.

ICP-OES or ICP-MS analysis of stocks and exposure media showed reasonable agreement with nominal concentrations, with some differences between $AgNO_3$ and Ag NPs. While $AgNO_3$ exposure stocks showed recoveries of 100 ± 0.0 % and 107 ± 0.9 %, for the 80 mg Ag L^{-1} and 10 mg Ag L^{-1}, respectively, Ag NP stocks were comparatively lower, with recoveries of 81.2 ± 0.0 % and 78.7 ± 22.2 %, for the 800 mg Ag L^{-1} and 100 mg Ag L^{-1}, respectively. In the Ag NP exposures, 84.9 ± 29.8 % and 64.4 ± 22.6 % of nominal Ag concentrations were recovered at T-0 and after 72 h, respectively, indicating no statistically significant reduction in recovery during the exposure period (t-test, $p = 0.18$).

To monitor changes in the behavior of silver during the exposure, a fractionation experiment was conducted at the beginning (T-0) and end (72 h) of the exposure (Figure 1). This was conducted in both the N2 and biosensor strains exposures. Findings from the N2 exposure are presented in Rossbach et al. (2019), and lay in accordance with results presented in the current article (Figure 1). No dissolved (<3 kDa) Ag fraction was found at either time point. It is highly probable that the positively charged Ag ions are associated with the negatively charged surface of the *E. coli*, and hence removed in the first centrifugation step, removing the aggregated fraction, before ultrafiltration. Overall, both forms of Ag show a propensity for aggregation and/or association with *E. coli* over the course of the exposure, as seen in the aggregated fraction (Figure 1). While larger, aggregated Ag particles might reduce the direct exposure of nematodes, Ag associated with *E. coli* might facilitate an increased dietary exposure. This coincides with the findings from

Kleiven et al. (2018). Assuming that Ag associated with *E. coli* is still capable of exerting a toxicological response, all toxicity results in the following sections are based on nominal concentrations in exposure suspensions.

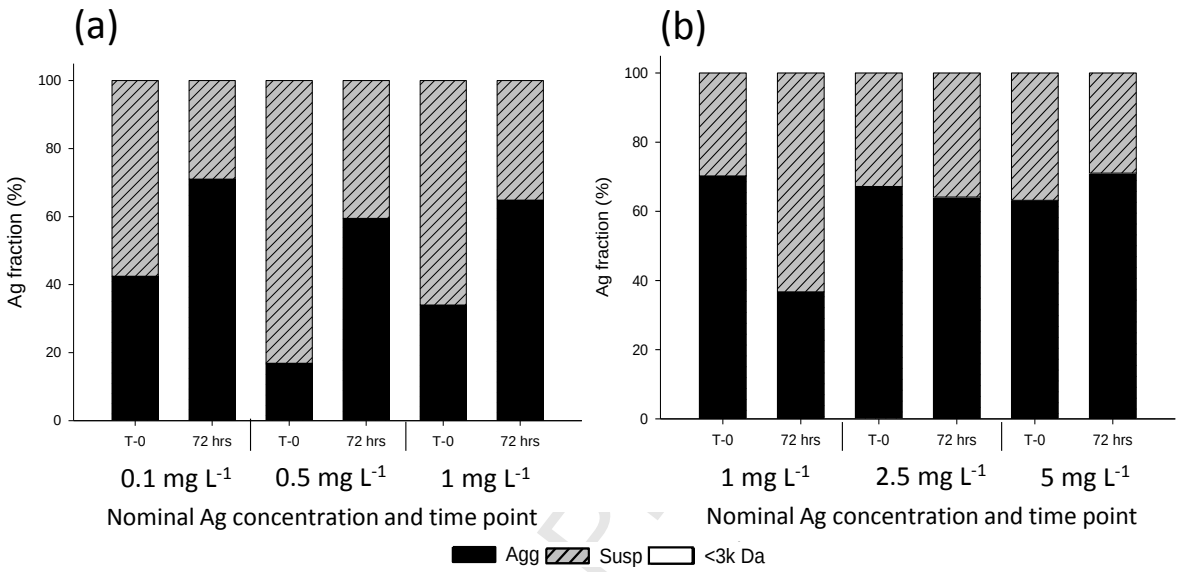

Figure 1. Characterization of the exposure media from the biosensor strain exposure, at T-0 and 72 h, showing the aggregated (Agg), suspended (Susp) and dissolved (< 3 kDa) Ag fraction of either $AgNO_3$ (a) or Ag NPs (b), in moderately hard reconstituted water containing *E. coli* and nematodes.

3.2. Dose-response toxicity test

The toxicity of $AgNO_3$ and Ag NPs was assessed in a standard 96 h toxicity test, in MHRW, by measuring growth, fertility and reproduction. No mortality was observed at any of the tested concentrations. $AgNO_3$ exposed nematodes displayed a dose dependent decrease in

growth with increasing concentrations (Figure 2a). All $AgNO_3$ concentrations up to 4 mg Ag L^{-1} showed statistically significant decrease in growth compared to controls, except for the lowest two concentrations. At 4 mg Ag L^{-1} a 56 % reduction in growth was found. These findings correspond to growth EC10 and EC50 estimations for $AgNO_3$ exposed nematodes of 0.34 mg Ag L^{-1} (95% CI 0.10 – 0.89) and 2.58 mg Ag L^{-1} (95% CI 1.82 – 3.77), respectively (Table 1). The Ag NP exposure on the other hand, resulted in no decrease in growth up to 5 mg Ag L^{-1}. This was followed by dose dependent reduction in development up to 40 mg Ag L^{-1} (ANOVA, $p < 0.05$), with a 51.2 % reduction in total body length compared to controls (n = 10). The EC10 and EC50 estimations are given in Table 1.

Similar to growth, fertility of nematodes exposed to $AgNO_3$ remained unaffected at 0.125 and 0.25 mg Ag L^{-1} (Figure 2b). A statistically significant reduction in fertility to 73 % of the control was observed at 0.5 mg Ag L^{-1} (ANOVA, $p = 0.008$), followed by a reduction to 28.1 % in nematodes exposed to concentrations of 1 mg Ag L^{-1} and 0 % fertility at 2 and 4 mg Ag L^{-1}. The impacts of Ag NP on fertility showed a reduction down to 83 % fertility at 5 mg Ag L^{-1} (Figure 2e), although this was not statistically significant from controls. Fertility was 0 % at concentrations ≥ 10 mg Ag L^{-1}.

Reproduction data for both $AgNO_3$ and Ag NP represents the most sensitive endpoint measured in the toxicity test. This was further confirmed by the EC10 and EC50 estimates (Table 1). At the lowest (0.125 mg Ag L^{-1}) $AgNO_3$ concentration a statistically significant (ANOVA, $p = 0.005$) decrease in reproduction, to below 35 % of that in controls, was measured (Figure 2c). At 0.5 mg Ag L^{-1} reproduction was less than 4% of that in controls (ANOVA, $p = 0.001$), followed by no reproduction at 1 mg Ag L^{-1} or higher. An impairment in

reproduction was observed in the Ag NP exposure, with a dose dependent reduction down to 12.6 % compared to controls at 5 mg Ag L^{-1} and a total absence of reproduction at concentrations ≥ 10 mg Ag L^{-1} (Figure 2f).

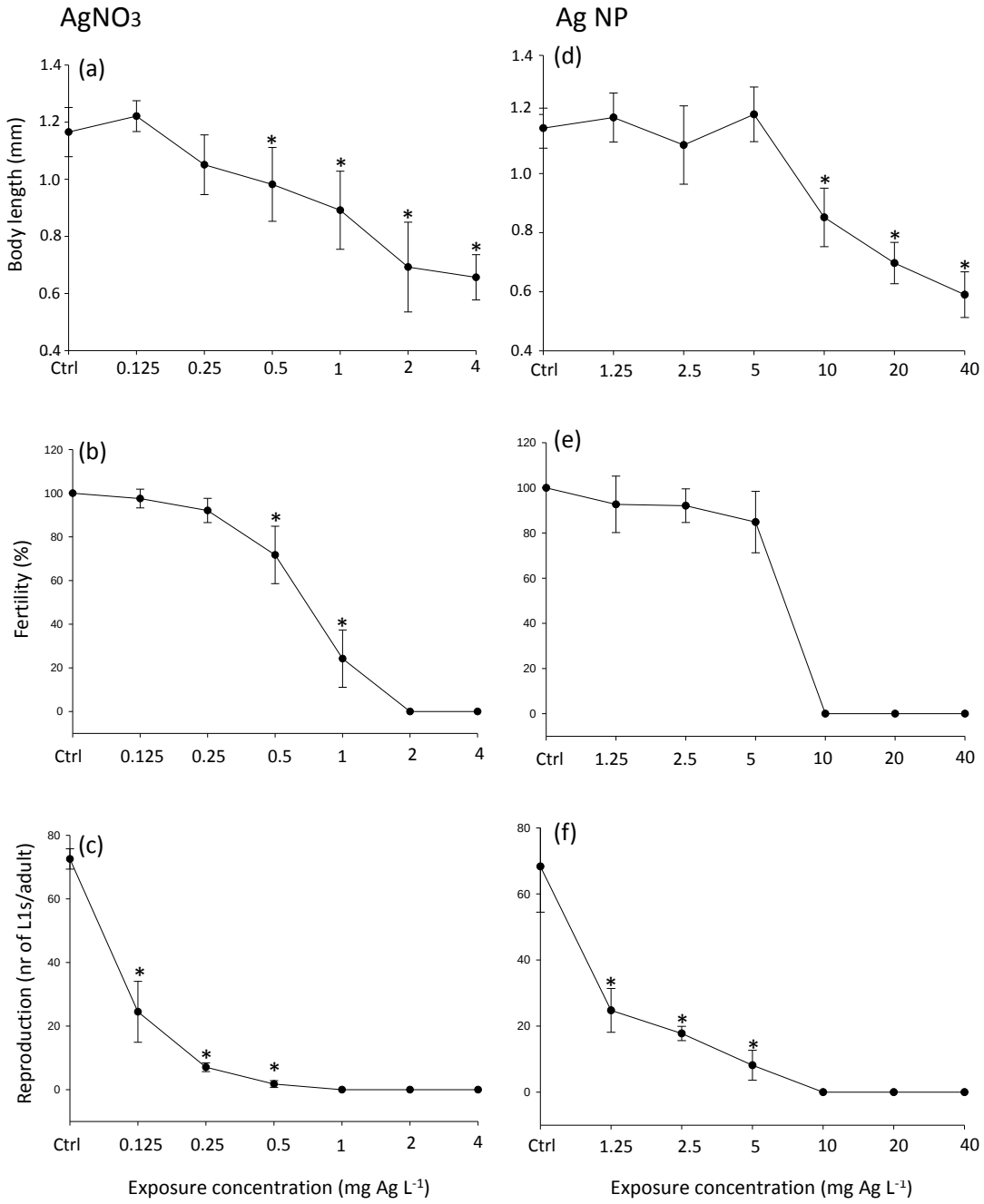

Figure 2. Growth (a and d), fertility (b and e) and reproduction (c and f) of *C. elegans*, exposed to either $AgNO_3$ or the Ag NPs NM300K, in MHRW containing *E. coli* in a standard 96 h toxicity test. Data is presented as mean ± SD (n = 10). Asterisks indicate significant differences (Tukey´s range test) between exposed nematodes and controls. Concentrations are given as nominal values.

Table 1. Reproduction, fertility and growth EC10 and EC50 values for *C. elegans* exposed to either $AgNO_3$ or Ag NPs in a standard 96 h toxicity test, in MHRW. 95 % confidence intervals are provided in parentheses. All values were calculated using the Hill model.

		$AgNO_3$ (mg Ag L^{-1})	**Ag NP (mg Ag L^{-1})**
Reproduction	**EC10**	0.04 (0.02 - 0.06)	0.11 (0.04 - 0.44)
	EC50	0.10 (0.07 - 0.12)	0.71 (0.41 - 1.21)
Fertility	**EC10**	0.33 (0.25 - 0.42)	3.50 (2.78 – 3.67)
	EC50	0.70 (0.59 - 0.79)	4.30 (3.90 – 4.45)
Growth	**EC10**	0.34 (0.10 – 0.89)	4.09 (1.51 – 8.30)
	EC50	2.58 (1.81 – 3.77)	18.6 (13.9 – 24.6)

3.3. ROS production and oxidative stress effects by $AgNO_3$ and Ag NPs

To investigate the potential role of free radicals in the toxic response observed in the N2 Bristol strain, three parallel tests were set up to obtain *in vivo* measurements of the effects of $AgNO_3$ and Ag NPs exposure on *sod*-1 gene expression and redox status, using the SOD-1 reporter strain, and the two biosensors HyPer and GRX. .

3.3.1. Concentration dependent increase in *sod-1* expression

For the investigation of *sod*-1 gene expression in *C. elegans* in response to $AgNO_3$ or Ag NP exposure, the GFP labelled reporter strain GA508 provides an accurate tool for the *in vivo* measurement of *sod-1* gene expression (Doonan et al., 2008). Superoxide is an intrinsic product of metabolism, and physiological *sod-1* expression increases, with increasing developmental stages (Doonan et al., 2008). In this study, the NM300K Ag NPs caused a dose dependent inhibition of development in the SOD-1 strain (Figure 3b and S4), which could potentially have an impact on *sod-1* response. Therefore, average intensity was normalized to the size of the nematodes in each exposure condition, to account for the decreased signal strength related to earlier developmental stages (Doonan et al., 2008).

The $AgNO_3$ exposed nematodes showed no statistically significant differences from controls at the lowest (0.1 mg Ag L^{-1}) exposure concentrations (ANOVA, $p = 0.7$), indicating no increase in Ag induced *sod-1* expression (Figure 3). However, a significant increase in *sod-1* expression for 0.5 and 1 mg Ag L^{-1} (ANOVA, $p = 0.01$ and $p < 0.001$) exposed nematodes, compared to controls was found. Similarly for the Ag NP exposed nematodes, no differences were found between controls and 1 mg Ag L^{-1} exposure (ANOVA, $p = 0.4$), however a statistically significant increase was seen for the 5 and 10 mg Ag L^{-1} Ag NP exposure (ANOVA, $p = 0.003$ and $p < 0.001$) (Figure 3a). Visual image analysis showed minor differences in the expression pattern of the intestine, pharynx and muscle tissue, between nematodes exposed to $AgNO_3$ or Ag NPs.

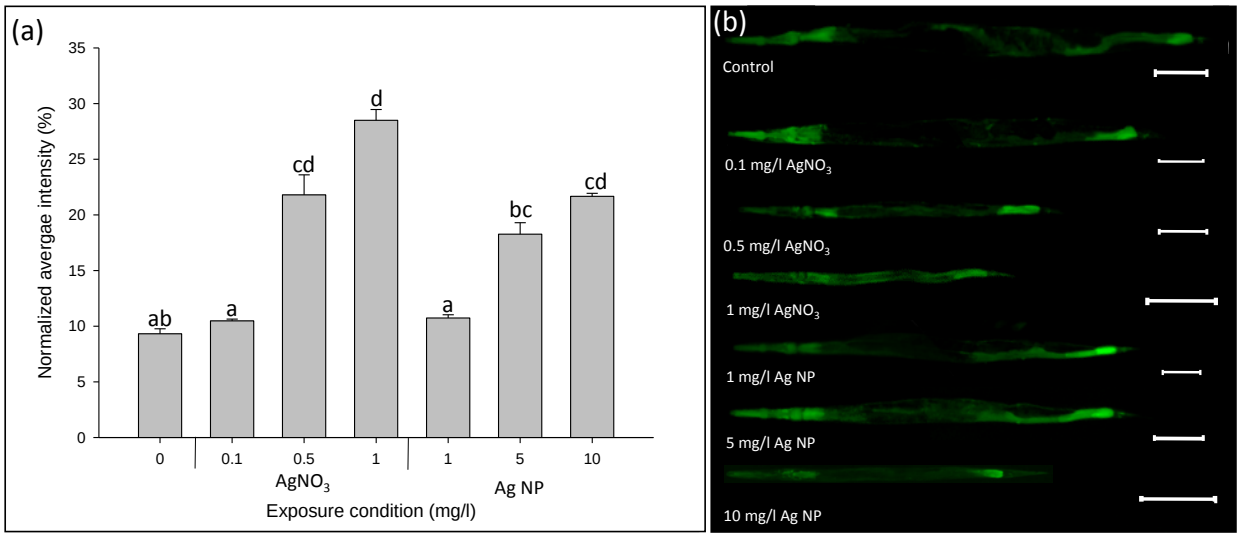

Figure 3. *In vivo* measurement of *sod*-1 expression pattern in the SOD-1 reporter strain GA508 (a) in response to either $AgNO_3$ or Ag NP exposure with corresponding images (b) (n = 10/concentration). Fluorescence average intensity values were normalized to nematode body size. Different letters indicate statistically significant differences among exposure groups. Bars represent 100 µm.

3.3.2. Exposure to Ag results in tissue specific cellular H_2O_2 production

The dismutation of O_2^- and $2H^+$ by superoxide dismutase antioxidant enzymes is the main source of H_2O_2 in the nematode (Back et al., 2012). Therefore, to quantify potential effects of this increase, the HyPer biosensor was employed in the current experiment. The dose response of HyPer was non-monotonous, unlike that observed from SOD-1. However, an overall significant increase compared to controls was seen from all Ag NP exposure concentrations ($p < 0.001$), while only the 1 mg Ag L^{-1} $AgNO_3$ exposure resulted in a significant increase ($p < 0.001$) (Figure 4a).

Controls expressed evenly low levels of H_2O_2 across the whole body, including the pharynx, intestine and tail, but no signal was seen in the gonads (Figure 4b). Notably, all Ag NP exposures appeared to cause pronounced increased H_2O_2 levels in the intestine, while $AgNO_3$ exposures increased H_2O_2 levels across the whole body, including the intestine, particularly at 1 mg Ag L^{-1} (Figure 4b). At 10 mg Ag L^{-1} Ag NP exposure, elevated H_2O_2 levels were also visible outside the intestine.

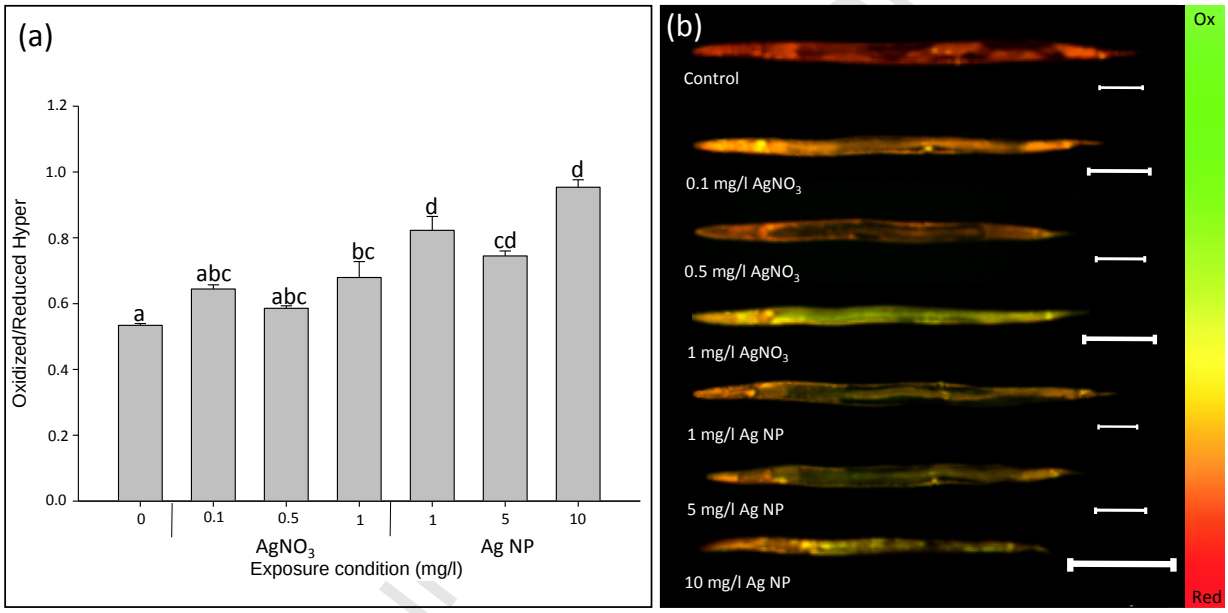

Figure 4. *In vivo* measurement (a) of the hydrogen peroxide biosensor HyPer in response to either $AgNO_3$ or Ag NP exposure with corresponding images (b) (n = 10 per concentration). Different letters indicate statistically significant differences among exposure groups. Bars represent 100 µm.

3.3.3. Nanoparticle exposure influences the GSSG/GSH redox status and oxidative stress in the intestine of *C. elegans*

One of the reducing agents of H_2O_2 in nematodes is glutathione (GSH) (Back et al., 2012). The GRX strain enables the measurement of the cellular GSSG/GSH redox balance in the nematode, and may thus serve as a proxy for *in vivo* measurement of oxidative stress (Back et al., 2012, Braeckman et al., 2016). In the current experiment, both $AgNO_3$ and Ag NPs resulted in statistically significant increases in oxidized to reduced GSSG/GSH ratios, compared to controls (Figure 5). Increases were significantly different from controls at 0.5 and 1 mg Ag L^{-1} $AgNO_3$ exposure ($p < 0.05$). Similarly, all three Ag NP exposure concentrations resulted in higher GSSG/GSH ratios compared to controls ($p < 0.001$). A visibly increased oxidation was seen in nematodes exposed to the higher $AgNO_3$ (0.5 and 1 mg Ag L^{-1}) and Ag NP (5 and 10 mg Ag L^{-1}) concentrations, compared to controls (Figure 5b). In all Ag concentrations, Ag NP showed a consistent pattern with increased oxidation primarily within the intestinal lining of the nematodes, similar to the pattern observed from the HyPer strain (Figure 4b). Notably, a significant concentration dependent growth effect and considerable variation between individual nematode GSSG/GSH ratios within exposure groups was observed (Figure 5).

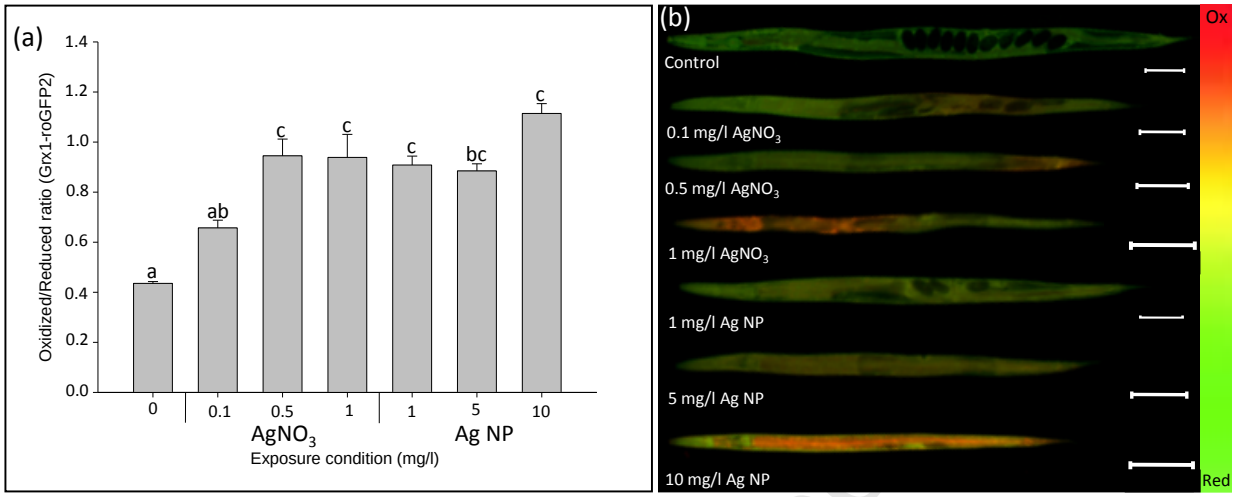

Figure 5. Oxidized to reduced ratios of the biosensor Grx1-roGFP2 (a) with corresponding images (b), measured *in vivo*, in response to the exposure to either $AgNO_3$ or Ag NPs (n = 10 per concentration). Different letters indicate statistically significant differences among exposure groups. Bars represent 100 µm.

Due to observable increases in oxidation in tissues connected to the lumen in both the GRX and HyPer strains, samples of the lumen, pharynx and tail were analyzed in detail for GSSG/GSH ratios, to identify variations in organ and tissue specific establishment of Ag induced oxidative stress (Figure 6a and b). Due to higher quality of the images, the quantification of tissue specific patterns was focused on the GRX strain. Compared to controls, all exposure concentrations resulted in increased GSSG/GSH ratios in the pharynx, intestinal lining, and the tail ($p < 0.05$) (Figure 6a). Both 1 mg Ag L^{-1} $AgNO_3$ (Figure 6c middle) and 10 mg Ag L^{-1} Ag NP (Figure 6c right) resulted in a comparable increase in oxidized to reduced ratios in the pharynx, compared to controls (figure 6c left). A significantly higher effect on redox status was measured in the luminal tissues from nematodes exposed to 1 and 10 mg Ag L^{-1} Ag NP (Figure 6d right), compared to controls

(Figure 6d left) and 1 mg Ag L^{-1} $AgNO_3$ (Figure 6d middle). In other parts of the body, there were no significant differences between the $AgNO_3$ and Ag NP exposures. However, during image analysis, it was noted that several nematodes exposed to either 0.5 or 1 mg Ag L^{-1} $AgNO_3$ had regions of elevated oxidized ratios, specifically in the head or the tail (Figure S4). This was not observed after Ag NP exposure.

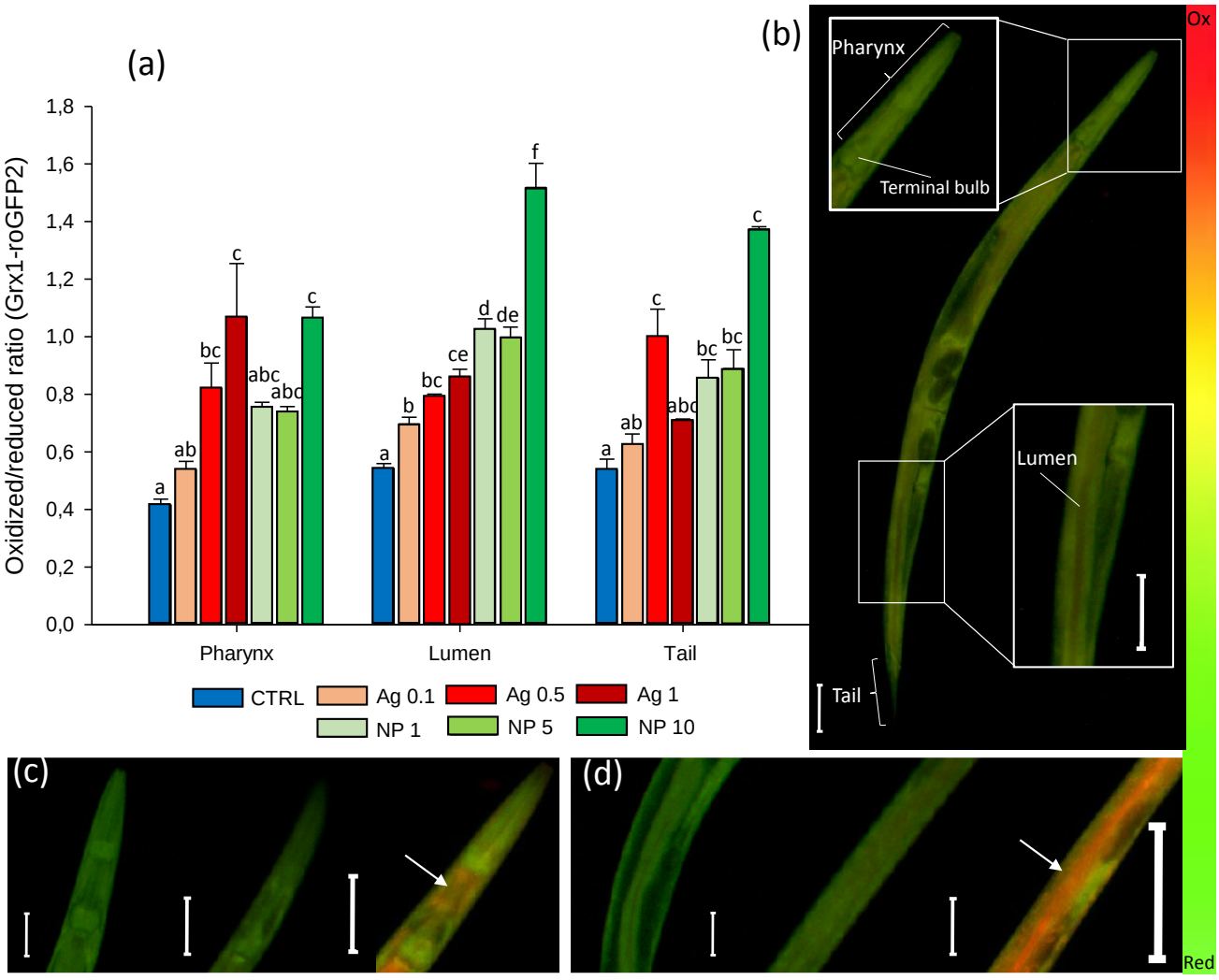

Figure 6. Spatial patterns of GSSG/GSH ratios within the nematode *C. elegans* taken from either control, $AgNO_3$ or Ag NP treatments (mean ± SEM, n = 5) (a). Measurements were made of the pharynx, a representative sample of the lumen, and the tail (b, 0.1 mg Ag L^{-1} Ag NP). Increased GSSG/GSH ratios were observed in all nematodes exposed to either $AgNO_3$ or Ag NPs, compared to controls, most significantly in the pharynx (c, from left to right: control, 1 mg Ag L^{-1} $AgNO_3$ and 10 mg Ag L^{-1} Ag NPs), and the lumen (d, from left to right: control, 1 mg Ag L^{-1} $AgNO_3$ and 10 mg Ag L^{-1} Ag NPs). Arrows indicate areas of interest with high levels of oxidation. Different letters indicate significant differences (ANOVA, $p < 0.05$). All scale bars are 50 μm in length.

4. Discussion

Although there is a consensus that ROS production and oxidative stress constitute important modes of action of NP induced toxicity, the mechanisms underlying cellular ROS generation are less well understood. There are two main ways by which NPs generate free radicals: either by acting as catalysts or indirectly via interference with metabolic processes (enzymes), which in turn leads to ROS formation (Huang et al., 2010). Moreover, ion release can contribute to the ROS mediated toxicity of certain NPs (Fabrega et al., 2011). Furthermore, there is little information on how NPs affect *in vivo* ROS production in the exposed organisms. In the current study, we capitalized on recent advances in Fluorescent Protein Sensors tagged *C. elegans* to investigate the effects of Ag NPs on redox biology in relation to toxic effects on development and reproduction, as measured in the N2 nematode strain.

4.1. NM300K Ag NPs and $AgNO_3$ affect cytosolic superoxide dismutase expression, hydrogen peroxide levels, and cellular redox balance

A number of studies have shown that NPs may affect cellular superoxide levels, particularly if mitochondrial function is compromised (Masoud et al., 2015, Abdal Dayem et al., 2017, Grzelak et al., 2018). By employing the GA508 SOD-1 reporter strain we were able to firmly demonstrate that NM300K Ag NPs induced *sod-1* superoxide antioxidant defense in a dose dependent manner (Figure 3), which unequivocally is a response to elevated cytosolic superoxide (Doonan et al., 2008). This suggests that either NM300K particles, released ions, or superoxide have been translocated from the lumen to the intracellular compartment. In previous studies, Ag ions on the particle surface, or their releases following dissolution, have been related to the increased ROS in response to Ag NP exposure (Carlson et al., 2008, Foldbjerg et al., 2009, Kim et al., 2009).

The observable differences in expression patterns in both intestine, pharynx and muscle tissues, suggest that $AgNO_3$ might be taken up more efficiently from the gastrointestinal tract and thereby cause higher superoxide production in tissues outside the intestine. The observation that both NM300K Ag NPs and $AgNO_3$ exposure generated excess superoxide demonstrates a significant potential to cause disturbance to physiological processes regulated by ROS signaling, and to cellular redox homeostasis. In line with these observations, we hypothesized that Ag generated superoxide would cause a downstream effect on ROS metabolism in *C. elegans*.

In normal physiological situation, sequestering of superoxide is the main source of H_2O_2 (Back et al., 2012, Braeckman et al., 2017). We therefore hypothesized that Ag induced *sod-*

1 expression would result in corresponding elevated cytosolic H_2O_2 as measured by the HyPer ratiometric biosensor. In this respect, the two exposure agents elicited different responses, where the NM300K NPs caused a much stronger production of H_2O_2 (Figure 4). The observation that H_2O_2 levels were, although not statistically significantly, lower in NM300K exposure at 5 mg Ag L^{-1}, compared to other exposure concentrations, could hint at the mobilization of antioxidant defenses, which successfully sequestered ROS to partially restore the redox homeostasis. However, antioxidant defenses seemed unable to counteract the total ROS burden at higher NM300K concentration, as evidenced by the increase in H_2O_2 at 10 mg Ag L^{-1}. Interestingly, the images suggested a gradient of H_2O_2 within the intestinal cells, with highest levels in tissues closest to the lumen (Figure 5b), which indicates tissue specific oxidative stress.

To test the hypothesis that increases in ROS, including H_2O_2, would influence the redox balance and produce oxidative stress in the nematodes, changes in the GSSG/GSH ratios were measured using the GRX biosensor strain. The results from the current study showed that the cellular redox potential was significantly impacted by the exposure to either form of Ag (Figure 5). This is in line with previous studies where Ag NPs were shown to increase ROS levels and deplete glutathione in rat liver cells and the fruit fly *Drosophila melanogaster* (Hussain et al., 2005, Ahamed et al., 2010). Moreover, Piao et al. (2011) showed that Ag NP may increase cellular ROS levels by directly inhibiting GSH synthesizing enzymes.

The compiled HyPer and GRX analysis indicates significant expenditure of glutathione to maintain cellular redox homeostasis, which enables the elimination of ROS, including H_2O_2.

The significant oxidation measured by the GRX strain at the highest exposure concentrations demonstrates a depletion of the glutathione pool, which strongly suggests that the antioxidant defense systems are overloaded.

4.2. Tissue specific oxidative stress effects in response to NM300K Ag NP exposure

Detailed analysis of specific tissues demonstrated distinct anatomical patterns of GSSG/GSH ratios, in a concentration dependent manner. This signifies a concentration dependent increased potential for oxidative stress damage. Results confirmed that the NM300K Ag NP exposure resulted in increased ROS generation, with high levels of oxidative stress, predominantly localized to the intestinal lumen (Figure 6). The substantially increased expression in tissues surrounding the lumen are in accordance with findings by Yang et al. (2014), who found Ag NP toxicity to act primarily in the intestine of the nematodes, whilst dissolved Ag was taken up by the intestinal cells, allowing for interferences with enzymes or organelles. Furthermore, Hunt et al. (2013) found Ag NPs (10 nm) to be primarily associated with the pharynx, lumen tissues and the intestine, where increases in exposure concentration did not significantly alter Ag NP localization.

The toxicity of nanoparticles is highly dependent on uptake and retention of the particles by the organism (Meyer et al., 2010). These parameters, however, are influenced by surface chemistry and hence reactivity, as well as by the size of the Ag NPs. Kleiven et al. (2018) showed high intake, but low retention of ~0.6 to 2% of the NM300K Ag NPs by *C. elegans* after depuration, indicating negligible levels of cellular internalization of the NM300K Ag

NPs. Differences in the uptake and internal distribution of the $AgNO_3$ compared to Ag NPs by the nematodes were also observed in the current study.

Potentially, ionic releases from the particles could result in intracellular uptake of Ag and cause toxic effects. Studies on the dissolution of uncoated NM300K Ag NPs showed time and media composition dependent ionic releases, varying between 0.07 – 29 % (Wasmuth et al., 2016, Köser et al., 2017). Nevertheless, the fractionation in the current study showed only low or no ionic fraction in either the beginning or following 72 h exposure, independent of the added form of Ag (Figure 1). In addition, the dissolution of NM300K NPs in the gut is kinetically not likely, given the very short passage time of the unretained particles in the gut of nematodes (<2 min) (McGhee and Ghafouri, 2007, Kleiven et al., 2018). It should be noted, however, that any dissolved Ag fraction released during the exposure in the media, may be subject to rapid sorption to the bacterial cells, and hence may therefore contribute to toxicity. In the current study, NM300K NPs induced oxidative stress in cells directly surrounding the gastrointestinal tract, indicating that, neither translocated NPs, nor the dissolved Ag fraction in the Ag NP exposure, produced any significant oxidative stress outside the intestine. Only at the highest exposure concentrations (10 mg Ag L^{-1} NM300K) was a slight oxidation visible in the anterior part of the nematode, surrounding the pharynx, as well as along the body outside the intestinal lumen (Figure 6d). Here, the observed increased oxidation may be attributed to either the cellular uptake of ROS, like $O_2^{\cdot-}$ and H_2O_2 produced on the surface of the particles, or translocation of the particles themselves (Goldstein et al., 2005, Choi et al., 2018).

In contrast, the results show that $AgNO_3$ exposure produced measurable levels of oxidation more evenly throughout the whole body of the nematodes (Figures 5 and 6). Although a low LMM Ag fraction and an overall increase in aggregated Ag fraction is observed in the $AgNO_3$ exposure media, internal dissolution of such aggregates may still be possible. Further, the lack of ionic fraction in the $AgNO_3$ exposure illustrates that any dissolved ions are likely to be removed by either sorption or precipitation, e.g. on the nematode's feed, *E. coli* (Kleiven et al., 2018). The fact that $AgNO_3$ is capable of inflicting oxidative damage (GRX strain) to most tissues in the entire nematode, however, could be indicative of Ag uptake into these cells (Connell et al., 1991, Ratte, 1999).

4.3. Ag induced redox effects in relation to toxic effects on development and reproduction

It has been suggested that organisms exposed to external ROS producers are able to reduce other biological processes, such as reproduction or biosynthesis, and instead increase antioxidant defense mechanisms (Lushchak, 2014). In the current study, both forms of Ag show a similar dose dependent response pattern in terms of growth, fertility and reproduction, however, NM300K Ag NP concentrations 5 - 10 fold higher than $AgNO_3$ were needed to produce similar levels of effect (Table 1, Figure 2). Regarding the genotypic response and cellular redox status, both $AgNO_3$ and NM300K produced a dose-dependent increase in ROS and oxidative stress. Notably, reproductive toxicity was observed at concentrations equal to or lower than those that induced the sod-1 antioxidant defense (Figures 2 and 3). At similar total Ag concentration (1 mg Ag L^{-1}), nematodes exposed to

NM300K exhibited a higher peroxide accumulation (*i.e.* larger imbalance of the cellular redox potential) than those exposed to $AgNO_3$.

This could suggest that nematodes fight ROS production by $AgNO_3$ more effectively than ROS produced by Ag NPs. In accordance with this, Mendes et al. (2015) found that $AgNO_3$ and NM300K Ag NPs induced different oxidative stress defense mechanisms in the springtail *Folsomia candida*, where both CAT and GST showed a clear particle specific effect. Their results also suggested a delayed reaction to the Ag NP exposure compared to $AgNO_3$, and a significantly reduced reproductive capacity for both forms of Ag. Similarly, results from the current study, suggest a relationship between oxidative stress development and reproductive toxicity from the Ag NP exposure, where increases in peroxide levels, as well as oxidative stress manifestation occur at Ag NP concentrations similar to those reducing reproduction. This is in contrast to the results from $AgNO_3$ exposure, where reproductive toxicity occurs at lower concentrations than those eliciting oxidative stress. Thus, results from the current study indicate differences in the toxic mode of action related to the reproductive toxicity of *C. elegans*, from the two forms of Ag, and a nano-specific tissue effect.

5. Conclusion

In the current study we addressed the toxicity of the NM300K Ag NPs compared to that of $AgNO_3$ and, through the application of the reporter strain SOD-1 and two biosensors HyPer and GRX, investigated changes in intracellular redox state in the nematode *C. elegans.* To the best of our knowledge, this is the first study to demonstrate nanoparticle-induced ROS production, induction of antioxidant defense and evidence of oxidative stress *in vivo* in live

organisms. Results showed that low concentrations of NM300K Ag NPs resulted in an imbalance in cellular redox potential, suggesting the manifestation of oxidative stress. It was also evident that NM300K Ag NPs induced superoxide production and triggered the expression of cytosolic *sod-1*. Furthermore, the Ag NP exposure increased cellular peroxide levels, and significantly changed the cellular redox balance. The stress patterns showed different distributions of oxidative stress within the organism, suggesting that in contrast to $AgNO_3$, Ag NPs predominantly act from within the lumen, presumably by interacting with the epithelium of intestinal cells. The compiled results on uptake, retention, toxic effects and oxidative stress patterns, consistently point to differences in modes of action between the two forms of Ag. Silver from $AgNO_3$ exposures may enter cells, inhibit enzymes, and perturb metabolic functions, which in turn leads to ROS production as a secondary effect, contributing to toxicity. For Ag NPs, and their transformation products, majorly confined to the lumen, ROS production and associated damage to the intestine and surrounding tissues appear to constitute the primary toxic mechanism.

6. Acknowledgements

The present study was funded by the NanoCharm (grant 221391) and NANoREG (grant 310584) projects. The reporter strain SOD-1 (GA508 wuls54[pPD95.77 sod-1::GFP, rol-6(su1006)]) was provided by Dr. Marina Ezcurra and Prof. David Gems from the Institute of Healthy Ageing Genetics (University College London). The biosensor strains Grx1-roGFP2 (GRX) and HyPer were provided by Dr. Braeckman from the Laboratory for Ageing Physiology and Molecular Evolution (University of Ghent, Belgium). For assistance with ICP

measurements, the authors thank K.A. Jensen and C. Lohne, and M. Kleiven and P. Lebed for technical support.

Conflict of Interest

The authors declare no conflict of interest.

7. References

ABDAL DAYEM, A., HOSSAIN, M. K., LEE, S. B., KIM, K., SAHA, S. K., YANG, G.-M., CHOI, H. Y. & CHO, S.-G. 2017. The Role of Reactive Oxygen Species (ROS) in the Biological Activities of Metallic Nanoparticles. *International Journal of Molecular Sciences,* 18**,** 120.

AHAMED, M., POSGAI, R., GOREY, T. J., NIELSEN, M., HUSSAIN, S. M. & ROWE, J. J. 2010. Silver nanoparticles induced heat shock protein 70, oxidative stress and apoptosis in Drosophila melanogaster. *Toxicol Appl Pharmacol,* 242**,** 263-9.

BACK, P., DE VOS, W. H., DEPUYDT, G. G., MATTHIJSSENS, F., VANFLETEREN, J. R. & BRAECKMAN, B. P. 2012. Exploring Real-Time in vivo Redox Biology of Developing and Aging Caenorhabditis elegans. *Free Radical Biology and Medicine,* 52**,** 850-859.

BRAECKMAN, B., BACK, P. U., MATTHIJSSENS, F. G. E., OLSEN, A. E. & GILL, M. S. E. 2017. Oxidative Stress. *In:* RATTAN, S. I. S. (ed.) *Healthy Ageing and Longevity.* Springer.

BRAECKMAN, B. P., SMOLDERS, A., BACK, P. & DE HENAU, S. 2016. In Vivo Detection of Reactive Oxygen Species and Redox Status in Caenorhabditis elegans. *Antioxidants & Redox Signaling,* 25**,** 577-592.

CARLSON, C., HUSSAIN, S. M., SCHRAND, A. M., BRAYDICH-STOLLE, L. K., HESS, K. L., JONES, R. L. & SCHLAGER, J. J. 2008. Unique Cellular Interaction of Silver Nanoparticles: Size-Dependent Generation of Reactive Oxygen Species. *Journal Physical Chemistry B,* 112**,** 13608-19.

CHOI, Y., KIM, H.-A., KIM, K.-W. & LEE, B.-T. 2018. Comparative Toxicity of Silver Nanoparticles and Silver Ions to Escherichia coli. *Journal of Environmental Sciences,* 66**,** 50-60.

CONNELL, D. B., SANDERS, J. G., RIEDEL, G. F. & ABBE, G. R. 1991. Pathways of silver uptake and trophic transfer in estuarine organisms. *Environmental Science & Technology,* 25**,** 921-924.

DOONAN, R., MCELWEE, J. J., MATTHIJSSENS, F., WALKER, G. A., HOUTHOOFD, K., BACK, P., MATSCHESKI, A., VANFLETEREN, J. R. & GEMS, D. 2008. Against the Oxidative Damage Theory of Aging: Superoxide Dismutases Protect Against Oxidative Stress but have Little or no Effect on Life Span in Caenorhabditis elegans. *Genes & Development,* 22**,** 3236-3241.

FABREGA, J., LUOMA, S. N., TYLER, C. R., GALLOWAY, T. S. & LEAD, J. R. 2011. Silver Nanoparticles: Behaviour and Effects in the Aquatic Environment. *Environment International,* 37**,** 517-531.

FOLDBJERG, R., OLESEN, P., HOUGAARD, M., DANG, D. A., HOFFMANN, H. J. & AUTRUP, H. 2009. PVP-coated silver nanoparticles and silver ions induce reactive oxygen species, apoptosis and necrosis in THP-1 monocytes. *Toxicol Lett,* 190**,** 156-62.

GOLDSTEIN, B. J., MAHADEV, K. & WU, X. 2005. Redox paradox: insulin action is facilitated by insulin-stimulated reactive oxygen species with multiple potential signaling targets. *Diabetes,* 54**,** 311-21.

GOMES, S. I. L., ROCA, C. P., SCOTT-FORDSMAND, J. J. & AMORIM, M. J. B. 2017. High-Throughput Transcriptomics Reveals Uniquely Affected Pathways: AgNPs, PVP-Coated AgNPs and Ag NM300K Case Studies. *Environmental Science: Nano,* 4**,** 929-937.

GRZELAK, A., WOJEWÓDZKA, M., MECZYNSKA-WIELGOSZ, S., ZUBEREK, M., WOJCIECHOWSKA, D. & KRUSZEWSKI, M. 2018. Crucial role of chelatable iron in silver nanoparticles induced DNA damage and cytotoxicity. *Redox Biology,* 15**,** 435-440.

HUANG, Y.-W., WU, C.-H. & ARONSTAM, R. S. 2010. Toxicity of Transition Metal Oxide Nanoparticles: Recent Insights from in vitro Studies. *Materials (Basel, Switzerland),* 3**,** 4842-4859.

HUNT, P. R., MARQUIS, B. J., TYNER, K. M., CONKLIN, S., OLEJNIK, N., NELSON, B. C. & SPRANDO, R. L. 2013. Nanosilver suppresses growth and induces oxidative damage to DNA in Caenorhabditis elegans. *Journal of Applied Toxicology,* 33**,** 1131-42.

HUSSAIN, S. M., HESS, K. L., GEARHART, J. M., GEISS, K. T. & SCHLAGER, J. J. 2005. In vitro toxicity of nanoparticles in BRL 3A rat liver cells. *Toxicol In Vitro,* 19**,** 975-83.

INTERNATIONAL ORGANIZATION FOR STANDARDIZATION, I. 2010. International Standard, Water Quality - Determination of the toxic effect of sediment and soil samples on growth, fertility and reproduction of Caenorhabditis elegans (Nematoda). *ISO 10872:2010.* Geneva, Switzerland.

JENSEN, K. A., BOOTH, A., KEMBOUCHE, Y. & BORASCHI, D. 2016. Validated Protocols for Test Item Preparation for Key in vitro and Ecotoxicity Studies, NANoREG Deliverable D2.06.

JIANG, J., OBERDÖRSTER, G. & BISWAS, P. 2009. Characterization of Size, Surface Charge, and Agglomeration State of Nanoparticle Dispersions for Toxicological Studies. *Journal of Nanoparticle Research,* 11**,** 77-89.

KIM, S., CHOI, J. E., CHOI, J., CHUNG, K. H., PARK, K., YI, J. & RYU, D. Y. 2009. Oxidative Stress-Dependent Toxicity of Silver Nanoparticles in Human Hepatoma Cells. *Toxicology In Vitro,* 23**,** 1076-84.

KIM, S. W., NAM, S. H. & AN, Y. J. 2012. Interaction of silver nanoparticles with biological surfaces of Caenorhabditis elegans. *Ecotoxicology and Environmental Safety,* 77**,** 64-70.

KLEIVEN, M., ROSSBACH, L. M., GALLEGO-URREA, J. A., BREDE, D. A., OUGHTON, D. H. & COUTRIS, C. 2018. Characterizing the behavior, uptake, and toxicity of NM300K silver nanoparticles in Caenorhabditis elegans. *Environmental Toxicology and Chemistry,* 37**,** 1799 - 1810.

KÖSER, J., ENGELKE, M., HOPPE, M., NOGOWSKI, A., FILSER, J. & THOMING, J. 2017. Predictability of Silver Nanoparticle Speciation and Toxicity in Ecotoxicological Media. *Environmental Science-Nano,* 4**,** 1470-1483.

LI, L., WU, H., JI, C., VAN GESTEL, C. A., ALLEN, H. E. & PEIJNENBURG, W. J. 2015. A metabolomic study on the responses of daphnia magna exposed to silver nitrate and coated silver nanoparticles. *Ecotoxicol Environ Saf,* 119**,** 66-73.

LIM, D., ROH, J. Y., EOM, H. J., CHOI, J. Y., HYUN, J. & CHOI, J. 2012. Oxidative Stress-Related PMK-1 P38 MAPK Activation as a Mechanism for Toxicity of Silver Nanoparticles to Reproduction in the Nematode Caenorhabditis elegans. *Environmental Toxicology and Chemistry,* 31**,** 585-92.

LUSHCHAK, V. I. 2014. Free Radicals, Reactive Oxygen Species, Oxidative Stress and its Classification. *Chemico-Biological Interactions,* 224**,** 164-75.

LÜERSEN, K., STEGEHAKE, D., DANIEL, J., DRESCHER, M., AJONINA, I., AJONINA, C., HERTEL, P., WOLTERSDORF, C. & LIEBAU, E. 2013. The Glutathione Reductase GSR-1 Determines Stress Tolerance and Longevity in Caenorhabditis elegans. *PLOS ONE,* 8**,** e60731.

MASOUD, R., BIZOUARN, T., TREPOUT, S., WIEN, F., BACIOU, L., MARCO, S. & HOUÉE LEVIN, C. 2015. Titanium Dioxide Nanoparticles Increase Superoxide Anion Production by Acting on NADPH Oxidase. *PloS one,* 10**,** e0144829-e0144829.

MCCORD, J. M. & FRIDOVICH, I. 1969. Superoxide Dismutase. An Enzymic Function for Erythrocuorein (Homecuprein) *Journal of Biological Chemistry,* 244**,** 6049-6055.

MCGHEE, J. & GHAFOURI, S. 2007. Bacterial residence time in the intestine of Caenorhabditis elegans. 9**,** 87.

MCSHAN, D., RAY, P. C. & YU, H. 2014. Molecular Toxicity Mechanism of Nanosilver. *Journal of food and drug analysis,* 22**,** 116-127.

MENDES, L., MARIA, V., SCOTT-FORDSMAND, J. & AMORIM, M. 2015. Ag Nanoparticles (Ag NM300K) in the Terrestrial Environment: Effects at Population and Cellular Level in Folsomia candida (Collembola). *International Journal of Environmental Research and Public Health,* 12**,** 12530.

MEYER, J. N., LORD, C. A., YANG, X. Y. Y., TURNER, E. A., BADIREDDY, A. R., MARINAKOS, S. M., CHILKOTI, A., WIESNER, M. R. & AUFFAN, M. 2010. Intracellular Uptake and Associated Toxicity of Silver Nanoparticles in Caenorhabditis elegans. *Aquatic Toxicology,* 100**,** 140-150.

NEL, A., XIA, T., MADLER, L. & LI, N. 2006. Toxic potential of materials at the nanolevel. *Science,* 311**,** 622-627.

PIAO, M. J., KANG, K. A., LEE, I. K., KIM, H. S., KIM, S., CHOI, J. Y., CHOI, J. & HYUN, J. W. 2011. Silver nanoparticles induce oxidative cell damage in human liver cells through inhibition of reduced glutathione and induction of mitochondria-involved apoptosis. *Toxicol Lett,* 201**,** 92-100.

POYNTON, H. C., LAZORCHAK, J. M., IMPELLITTERI, C. A., BLALOCK, B. J., ROGERS, K., ALLEN, H. J., LOGUINOV, A., HECKMAN, J. L. & GOVINDASMAWY, S. 2012. Toxicogenomic Responses of Nanotoxicity in Daphnia magna Exposed to Silver Nitrate and Coated Silver Nanoparticles. *Environmental Science & Technology,* 46**,** 6288-6296.

RATTE, H. T. 1999. Bioaccumulation and toxicity of silver compounds: A review. *Environmental Toxicology and Chemistry,* 18**,** 89-108.

RIBEIRO, M. J., MARIA, V. L., SCOTT-FORDSMAND, J. J. & AMORIM, M. J. B. 2015. Oxidative Stress Mechanisms Caused by Ag Nanoparticles (NM300K) are Different from Those of AgNO(3): Effects in the Soil Invertebrate Enchytraeus crypticus. *International Journal of Environmental Research and Public Health,* 12**,** 9589-9602.

ROH, J. Y., SIM, S. J., YI, J., PARK, K., CHUNG, K. H., RYU, D. Y. & CHOI, J. 2009. Ecotoxicity of Silver Nanoparticles on the Soil Nematode Caenorhabditis elegans Using Functional Ecotoxicogenomics. *Environmental Science & Technology,* 43**,** 3933-3940.

ROSSBACH, L. M., MAREMONTI, E., EIDE, D. M., OUGHTON, D. H. & BREDE, D. A. 2019. Adaptive tolerance to multigenerational silver nanoparticle (NM300K) exposure by the nematode Caenorhabditis elegans is associated with increased sensitivity to AgNO3. *Nanotoxicology***,** 1-16.

SCHAFER, F. Q. & BUETTNER, G. R. 2001. Redox environment of the cell as viewed through the redox state of the glutathione disulfide/glutathione couple. *Free Radical Biology and Medicine,* 30**,** 1191-1212.

SYAFIUDDIN, A., SALMIATI, SALIM, M. R., BENG HONG KUEH, A., HADIBARATA, T. & NUR, H. 2017. A Review of Silver Nanoparticles: Research Trends, Global Consumption, Synthesis, Properties, and Future Challenges. *Journal of the Chinese Chemical Society,* 64**,** 732-756.

TOWNSEND, D. M., TEW, K. D. & TAPIERO, H. 2003. The importance of glutathione in human disease. *Biomed Pharmacother,* 57**,** 145-55.

UNITED STATES ENVIRONMENTAL PROTECTION AGENCY, U. E. 2002. Methods for Measuring the Acute Toxicity of Effluents and Receiving Waters to Freshwater and Marine Organisms, 5th edition. EPA-821-R-02-012. Office of water, Washington DC, USA.

VAN DER PLOEG, M. J. C., HANDY, R. D., WAALEWIJN-KOOL, P. L., VAN DEN BERG, J. H. J., RIVERA, Z. E. H., BOVENSCHEN, J., MOLLEMAN, B., BAVECO, J. M., TROMP, P., PETERS, R. J. B., KOOPMANS, G. F., RIETJENS, I. & VAN DEN BRINK, N. W. 2014. Effects of silver nanoparticles (NM-300K) on

Lumbricus rubellus earthworms and particle characterization in relevant test matrices including soil. *Environmental Toxicology and Chemistry,* 33**,** 743-752.

VINDIMIAN, E., 2016. RegTox [cited 2020 January 06]. Available from: http://www.normalesup.org/~vindimian/en_index.html.

VÖLKER, C., KÄMPKEN, I., BOEDICKER, C., OEHLMANN, J. & OETKEN, M. 2015. Toxicity of Silver Nanoparticles and Ionic Silver: Comparison of Adverse Effects and Potential Toxicity Mechanisms in the Freshwater Clam Sphaerium corneum. *Nanotoxicology,* 9**,** 677-685.

WASMUTH, C., RÜDEL, H., DÜRING, R.-A. & KLAWONN, T. 2016. Assessing the suitability of the OECD 29 guidance document to investigate the transformation and dissolution of silver nanoparticles in aqueous media. *Chemosphere,* 144**,** 2018-2023.

WU, G., FANG, Y.-Z., YANG, S., LUPTON, J. R. & TURNER, N. D. 2004. Glutathione Metabolism and Its Implications for Health. *The Journal of Nutrition,* 134**,** 489-492.

YANG, X., JIANG, C., HSU-KIM, H., BADIREDDY, A. R., DYKSTRA, M., WIESNER, M., HINTON, D. E. & MEYER, J. N. 2014. Silver Nanoparticle Behavior, Uptake, and Toxicity in Caenorhabditis elegans: Effects of Natural Organic Matter. *Environmental Science & Technology,* 48**,** 3486-3495.

ZHAO, C. M. & WANG, W. X. 2011. Comparison of acute and chronic toxicity of silver nanoparticles and silver nitrate to Daphnia magna. *Environmental Toxicology & Chemistry,* 30**,** 885-92.

CRediT Author Statement

Lisa M. Rossbach: Conceptualization, Methodology, Formal Analysis, Writing – Original Draft, Writing – Review & Editing

Deborah H. Oughton: Conceptualization, Resources, Supervision, Writing – Review & Editing, Funding acquisition

Erica Maremonti: Methodology, Validation, Writing – Review & Editing

Claire Coutris: Methodology, Writing – Review & Editing, Visualization

Dag A. Brede: Conceptualization, Methodology, Supervision, Writing – Original Draft, Writing – Review & Editing

Declaration of interests

☒ The authors declare that they have no known competing financial interests or personal relationships that could have appeared to influence the work reported in this paper.

☐The authors declare the following financial interests/personal relationships which may be considered as potential competing interests:

Graphical abstract

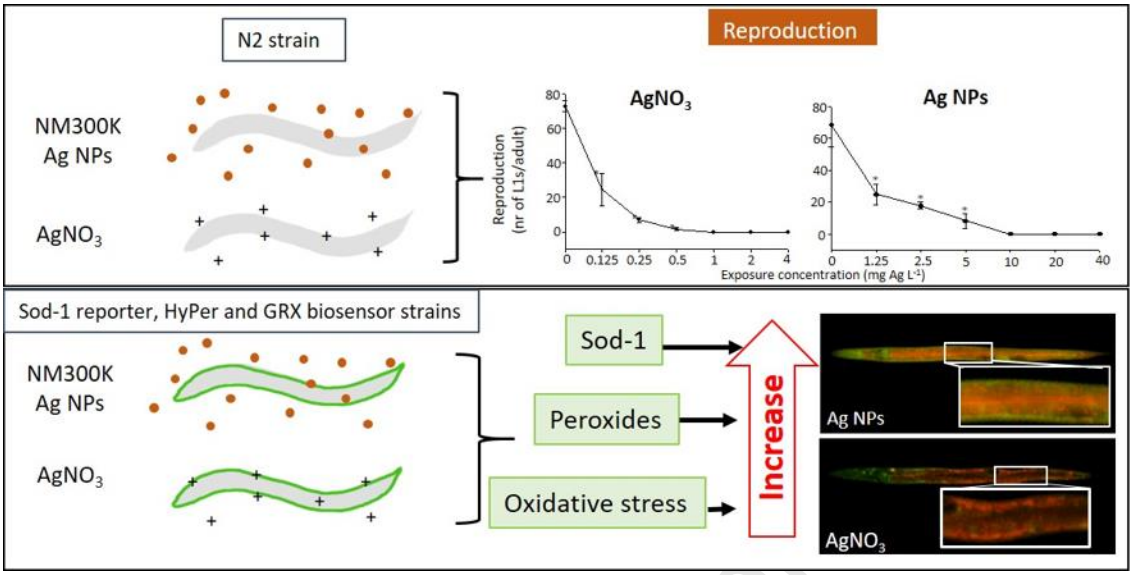

Highlights

- NM300K Ag NPs driven oxidative stress was analyzed *in vivo* in nematodes
- Contrasting body distributions of oxidative stress were found with $AgNO_3$ and NM300K
- Differences in Ag retention and body distribution governed oxidative stress patterns
- $AgNO_3$ caused uniform tissue and cell redox imbalance
- ROS damages by NM300K were confined to the luminal tissues